

Article

Spatiotemporal Dissolved Silicate Variation, Sources, and Behavior in the Eutrophic Zhanjiang Bay, China

Peng Zhang ^{1,2}, Jia-Lei Xu ¹, Ji-Biao Zhang ^{1,2,*}, Jian-Xu Li ¹, Yan-Chan Zhang ¹, Yi Li ¹ and Xin-Qi Luo ¹

¹ College of Chemistry and Environmental Science, Guangdong Ocean University, Zhanjiang 524088, China; zhangpeng@gdou.edu.cn (P.Z.); xujialei2@stu.gdou.edu.cn (J.-L.X.); lijianxu@stu.gdou.edu.cn (J.-X.L.); zhangyanchan@stu.gdou.edu.cn (Y.-C.Z.); liyi7@stu.gdou.edu.cn (Y.L.); 201711314121@stu.gdou.edu.cn (X.-Q.L.)

² Southern Laboratory of Ocean Science and Engineering (Guangdong Zhanjiang), Zhanjiang 524088, China

* Correspondence: zhangjb@gdou.edu.cn; Tel.: +86-0759-238-3311

Received: 26 October 2020; Accepted: 16 December 2020; Published: 21 December 2020



Abstract: Dissolved silicate (DSi) is an important nutrient in coastal water, which is used by planktonic diatoms for cell division and growth. In this study, surface water samples were collected in the eutrophic Zhanjiang Bay (ZJB) in 2019, covering a seasonal variation of coastal water and land-based source water discharge. The spatiotemporal DSi distribution, land-based sources flux input and behaviors in ZJB were studied and discussed. The results show that the DSi concentration had significant differences in spatiotemporal scale. The average concentration of DSi in ZJB was $38.00 \pm 9.48 \mu\text{mol}\cdot\text{L}^{-1}$ in spring, $20.23 \pm 11.27 \mu\text{mol}\cdot\text{L}^{-1}$ in summer, $12.48 \pm 1.42 \mu\text{mol}\cdot\text{L}^{-1}$ in autumn and $11.96 \pm 4.85 \mu\text{mol}\cdot\text{L}^{-1}$ in winter. The spatiotemporal DSi distribution showed a decreasing gradient from the top to the mouth of ZJB, which was affected by land source inputs and hydrodynamics. The land-based sources' input concentration of DSi in ZJB ranged from 0.021 to $0.46 \text{ mol}\cdot\text{L}^{-1}$, with an average of $0.14 \text{ mol}\cdot\text{L}^{-1}$, and the total annual flux of DSi was $1.06 \times 10^9 \text{ mol}$, comprising up to 8.28%, 41.55% and 50.17% in dry, normal, and wet seasons, respectively. The Suixi River contributed the highest DSi flux proportion in all seasons. The DSi in land-based source water was mainly affected by water flow discharge, diatom uptake and impacts from anthropogenic activities. Compared with dissolved inorganic nitrogen (DIN) and dissolved inorganic phosphorus (DIP), the DSi was the limitation nutrient in ZJB. Additionally, the DSi concentration in the coastal water was negatively correlated with salinity. The seasonal DSi/DIN and DSi/DIP ratios in land-based sources discharge water was significantly higher than that in coastal water ($p < 0.05$). Land-based sources of DSi input played an important role in nutrients composition that sustained diatoms as the dominant species in ZJB.

Keywords: spatiotemporal variation; dissolved silicate; land-based sources; coastal water; Zhanjiang bay

1. Introduction

Silicon is the second most abundant element in the Earth's crust and is one of the major constituents in seawater, where it is present in both dissolved and particulate form [1]. Dissolved silicate (DSi) is a vital nutrient required by diatoms for growth in coastal water [2–4]. Diatoms are one of the most important primary producers in the ocean, contributing more than 40% of global marine primary production [5,6]. Silicon plays a very important role in regulating the community composition of phytoplankton [7–9]. The excess riverine dissolved inorganic nitrogen (DIN) and dissolved inorganic phosphorus (DIP) resulting from agriculture, industry and domestic wastewater inputs, has led to a

shift in the Si:N:P ratio in recent years [10–12]. As a result, the relatively excess N and P source input could lead to the decline in Si/N and Si/P in coastal water [10–12]. Diatoms use DSi to form a silicified cell wall composed of amorphous silica also referred to as biogenic silica (BSi) [11,12]. The availability of DSi and its relative abundance compared to the other nutrients can influence the composition of the phytoplankton community, which can subsequently affect the ecological functioning of the ecosystem [9,11,13,14]. Meanwhile, it controls N and P nutrient ratios and planktonic blooms in the aquatic ecosystem [12,15]. As it is closely related to the ocean carbon cycle and biological pumps, the research on the biogeochemical behavior of silicon has attracted people's attention during recent years [2,12,16–19].

Land chemical weathering of silicate minerals can provide rivers with a large amount of DSi [17]. Rivers carrying a large amount of DSi will then flow into the coastal water [20,21]. About 80% of the net input of DSi into the world's oceans each year comes from rivers' input [22]. The land–ocean transition zone plays a key role in silica biogeochemistry [23]. The biogeochemical behavior of nutrients in the estuary area, such as whether it is conservative or not, has a decisive effect on its output. It is important in the biogeochemical cycle [24–27]. The amount of DSi entering marine waters directly impacted the abundance and community composition of phytoplankton species assemblages [12,28]. In recent decades, anthropogenic perturbations have impacted upon the silicon cycle at the global scale [1,29–31]. For example, dam construction will decrease DSi in aquatic systems, which has been observed worldwide [1,14,32,33]. A series of studies have shown that hydrological alterations have changed DSi loads to the sea, with adverse effects on the ecosystem [34–36]. For example, the eutrophication and red tides caused by the nutrients' increase and nutrients' composition change in the East China Sea are one of the abnormal phenomena in marine environment in recent years [12,13,37]. The increases in DIN/DSi and DIN/DIP ratios have likely induced the succession of *S. costatum* to *P. donghaiense* and inspired the potential for silicon to act as a limiting nutrient in the East China Sea [12,37,38]. Therefore, under the pressure of increased human activities and climatic change, understanding DSi distribution, biogeochemical behaviors in coastal water and the factors controlling land-based DSi sources flux export from land to coast is crucial to obtaining a better insight into the impacts of nutrient dynamics on aquatic ecosystems [39,40].

Zhanjiang Bay (ZJB) is located in the southernmost part of the Chinese mainland, in Leizhou Peninsula, Guangdong Province. The eutrophic coastal water is largely a consequence of land-based nutrient input [40–42]. During the past three decades, there have been many sewage outlets of municipal sewage treatment plants along the coast and a large amount of industrial wastewater is discharged into the bay, which leads to the current situation of eutrophication [41]. The marine ecosystem has shifted from a P-limited oligotrophic state before the 1980s to a N-limited eutrophic state in ZJB. Red tides rarely occurred before the 1980s, but have occurred periodically and frequently since the 1990s. ZJB, where nine red tides were identified during the period of 2010–2019 compared to six times during the period of 2000–2009 [43]. Additionally, the red tide's phytoplankton composition was diatom-dominated species in recent decades [43]. Previous studies have been conducted on the eutrophication problem of ZJB and adjacent estuary waters, especially focused on the distributions and changes of dissolved inorganic nitrogen, dissolved inorganic phosphorus, and dissolved oxygen [44,45]. Compared with land-based sources of nitrogen and phosphorus, the land-based source of DSi was not conducted in ZJB. Additionally, compared with the DSi in Bohai, the Yellow Sea and the East China Sea [12,46], the effects of spatiotemporal variation, land-based sources input, and behavior of DSi in eutrophic ZJB of South China Sea are still poorly known.

Given the key role of biogeochemical Si distribution and behavior in the coastal ecosystem under the land-based sources input, a land–ocean integrated field investigation was performed to understand spatiotemporal variation, land-based sources' input, and the behavior of DSi in eutrophic ZJB. We conducted field investigations in ZJB in 2019 to determine the concentration in land-based sources and coastal water of ZJB, and related environmental factors were also analyzed. The aim of this study is to explore spatiotemporal DSi variation, sources, and behavior in the eutrophic ZJB.

This study provides the first assessment of how spatiotemporal DSi dynamics in coastal water respond to increased land-based sources' input in ZJB and understand the DSi behavior in aquatic systems.

2. Materials and Methods

2.1. Study Area and Monitoring Stations

ZJB is a semi-enclosed bay that is connected to the South China Sea through a narrow channel of approximately 2 km in length. The bay has a surface area of 193 km² and an average water depth of approximately 18 m (Figure 1). There are more than 5 small seasonal rivers and sewage outlets carrying various amounts of water into the coastal water. Among these rivers are the Suixi River, Nanliu River, Lvtang River, Wenbao River and Hongxing river, of which the largest is the Suixi River, located at the top of ZJB [41,42]. However, with the rapid socioeconomic development of Zhanjiang city, most of these rivers have become polluted with agricultural, industrial, and domestic wastewater from the land-based sources adjacent to the area of ZJB. In addition, there are many aquaculture areas surrounding ZJB, which also contribute some the land-based sources' load input. During the past three decades, the frequency of red tide outbreak in ZJB increased significantly. The frequency of red tide outbreak was two in 2005, which had the biggest accumulative area of red tide outbreak, with 310 km² [42]. Data from the monitoring stations of seawater and survey stations of the estuaries and sewage outlets of terrestrial input were collected in ZJB (Figure 1). Water sampling was chosen with respect to the physical–chemical–biological status of the hydrological and land-based source input's spatial distribution characteristics in ZJB (Figure 1). Sampling of land-based sources and seawater was conducted in the same seasonal period [42]. Monitoring stations of seawater in ZJB were selected in accordance with the method specified in the Specification of Oceanographic Survey [47].

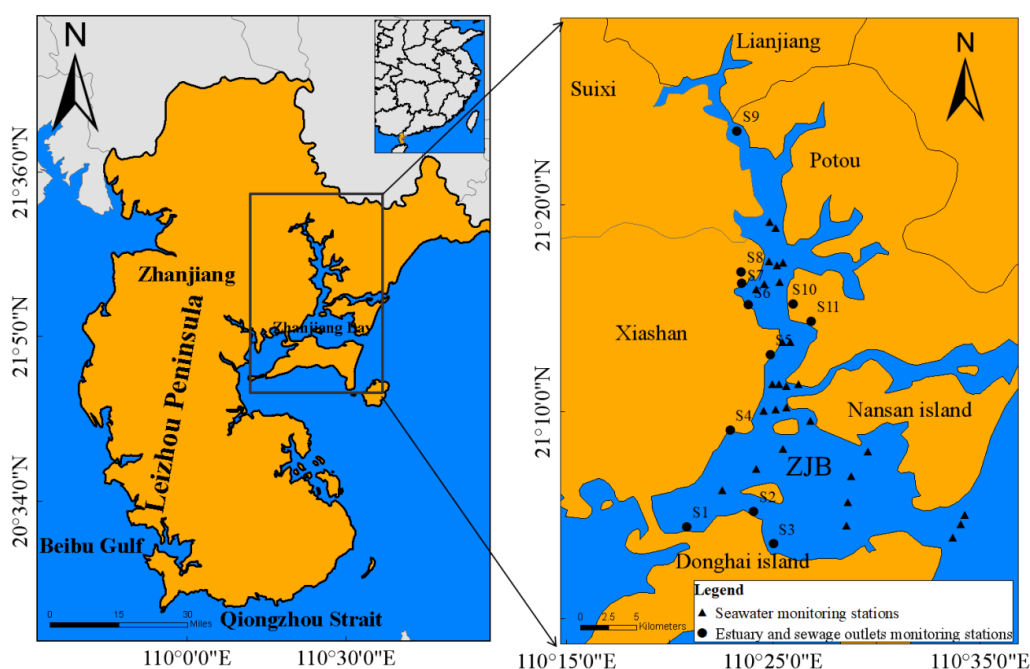


Figure 1. Geographic location, land-based sources, and coastal water monitoring stations in Zhanjiang Bay.

2.2. Field Sampling Method

In field sampling, the normal season was 20 April 2019, 11 January 2019 represented the dry season, and 4 July 2019 represented the wet season. The method of collection, preservation, and measurement of river water and sewage water samples was performed in accordance with the Technical Specification Requirements for Monitoring of Surface Water and Waste Water [48]. According to the Code for

liquid flow measurement in open channels (GB50179-93), water samples were collected using a portable sampler, and a rotor flow meter was used to monitor the flow of each river into the sea simultaneously [49]. During the investigation period, sewage outlets 8 and 11 from the flood gate into the sea (Table 1) and breeding sewage outlet in the sloping head area of Binhu Park were both closed, so there were no water samples in July (wet season). In January 2019 (winter), April (spring), June (summer) and November (autumn), water samples were collected from the surface coastal water in ZJB. After transportation to the laboratory, all samples were immediately filtered with a 0.45 µm pore-size acetate cellulose filter membrane within 2 h [50], and then the water samples were stored in plastic bottles which were cleaned with diluted hydrochloric acid (pH 2) overnight, then rinsed with ultrapure water (Resistivity = 18.25 MΩ·cm) to neutral pH. The samples were frozen in a refrigerator (−18 °C) before analysis within one week. When samples were thawed prior to analysis, sufficient time (preferably >24 h) was allowed for depolymerization [51]. A subset of samples were analyzed before and after freezing to ensure the freezing and thawing process had no impact on DSi concentrations, with no significant differences measured (samples with 10%).

Table 1. Investigation of estuaries and sewage outlets.

Station	Estuaries and Sewage Outlets	Longitude/°	Latitude/°
S1	Donghai island aquaculture sewage outlet 1	110.347778	21.073889
S2	Donghai island aquaculture sewage outlet 2	110.401667	21.086389
S3	Hongxing estuary	110.4175	21.060278
S4	Nanliu river estuary	110.3825	21.151944
S5	Lvtang river estuary	110.414722	21.212778
S6	Wenbao river estuary	110.397222	21.253056
S7	Jinsha Bay sewage outlet	110.391944	21.270278
S8	Sewage outlet of flood control sluice in Binhu park	110.391389	21.279167
S9	Suixi river estuary	110.388056	21.392778
S10	Sewage outlet of flood control sluice in Dengta park	110.433056	21.253611
S11	Potou primary school estuary	110.448056	21.239722

2.3. Analysis Methods

The analysis of the samples is in accordance with the fourth part of “Marine Monitoring Standard-Seawater Analysis GB17378.4-2007”: Seawater analysis standard operation. DSi analysis was performed using silicon molybdate blue method via spectrophotometric determination (MAPADA, UV-1100) [47]. The detection limit was 0.09 µmol·L^{−1} for DSi. The measurement blank of sampling water bottle was 0.00 µmol·L^{−1} for DSi. The precision was estimated to be better than 5% by repeated determinations of 10% of the samples. In each batch of samples, the standard solution from the Institute of Standard Samples of the Ministry of Environmental Protection of The People’s Republic of China was used for labeling recovery to ensure the accuracy of test results (2%).

2.4. Method of Quantifying Land-based Sources DSi Flux

DSi export was estimated from the ZJB land-based sources, representing the DSi fluxes from the most downstream main-channel station with water discharge data. Thus, river estuaries’ and sewage outlets’ monitoring stations were used to quantify the fluxes of DSi transported from the river estuaries and sewage outlets to the coastal water. The annual riverine and sewage outlets flux of DSi used here were estimated using the equation [41,42]—the calculation formula of the sea flux is as follows:

$$F_i = \sum C_{i,j} Q_{i,j}$$

where F_i (mol) is the seasonal flux of the DSi in land-based source i ; $C_{i,j}$ (mol·m^{−3}) is the average concentration of the DSi in the land-based source i during month j ; and $Q_{i,j}$ (m³) is the cumulative discharge of land-based source i during month j .

2.5. Statistical Analysis

The geographic information system ArcGIS (10.2) was used to draw the schematic diagram of monitoring stations in the estuary and sewage outlets of ZJB from land-sources to the sea; the DSi pollutant concentration composition and marine flux were mapped by OriginLab, Origin (9.0) software. The ocean data view (ODV) was used to draw the DSi spatiotemporal distribution by weighted-average gridding interpolation method [52]. Linear regression analysis was used to analyze the relationships between seasonal DSi concentration salinity. Significant differences in the DSi concentrations among different seasons were assessed by one-way ANOVA ($p < 0.05$). The data were analyzed by Excel software, and the data were expressed as arithmetic (Mean \pm SD).

3. Results

3.1. Spatiotemporal DSi Variation in the ZJB Coastal Water

There were significant differences in the concentration distribution of DSi in ZJB ($p < 0.05$) (Figures 2 and 3). The concentration of DSi was higher especially in the Potou area and Suixi coastal waters ($29.34 \mu\text{mol}\cdot\text{L}^{-1}$) than others in April 2019 (spring). (Figure 2). The concentration of DSi ($3.57 \mu\text{mol}\cdot\text{L}^{-1}$) was lower at the bay mouth than others in January (winter). The concentration of DSi was higher in Potou and Xiashan than in the other areas during the autumn and summer, which was the main features. Meanwhile, the horizontal distribution of DSi in January had a similar trend. DSi concentration was the lowest in the bay mouth. The distribution of DSi concentration levels in November (autumn) 2019 was similar to the former three months (Figure 2).

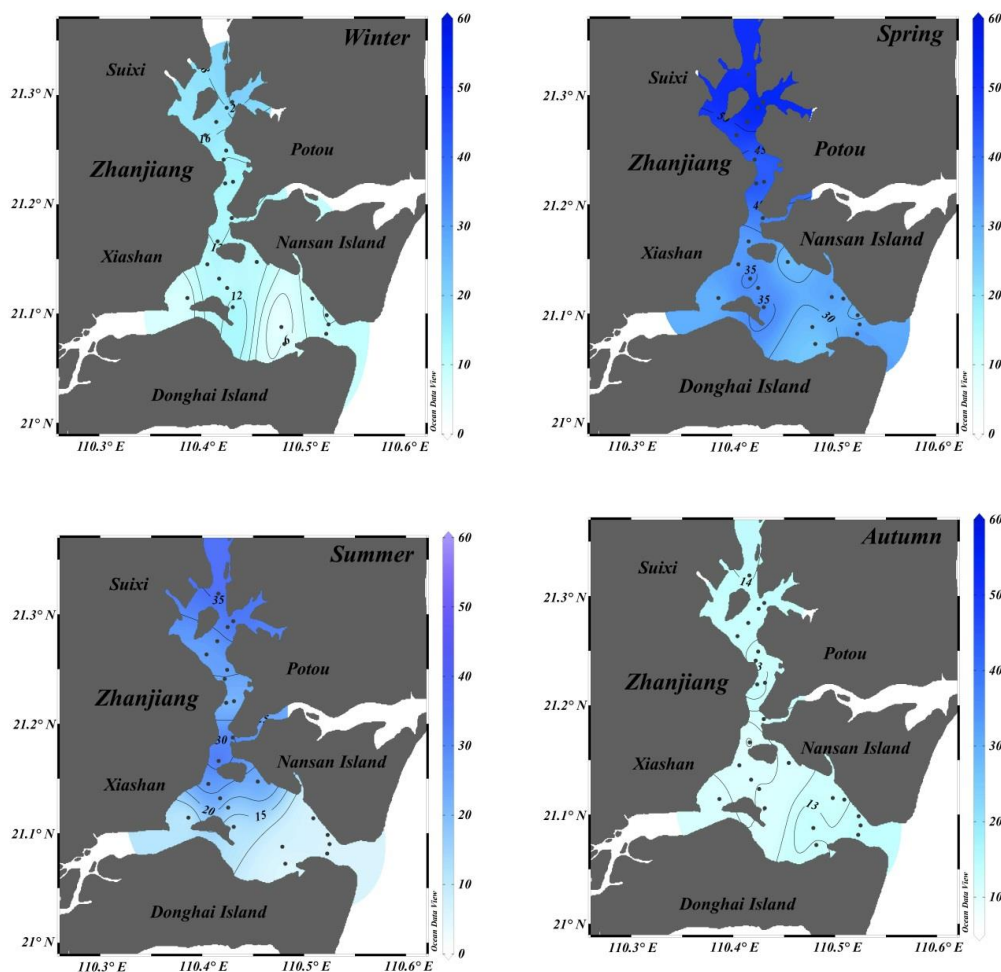


Figure 2. Spatiotemporal dissolved silicate (DSi) distribution in the Zhanjiang Bay coastal water.

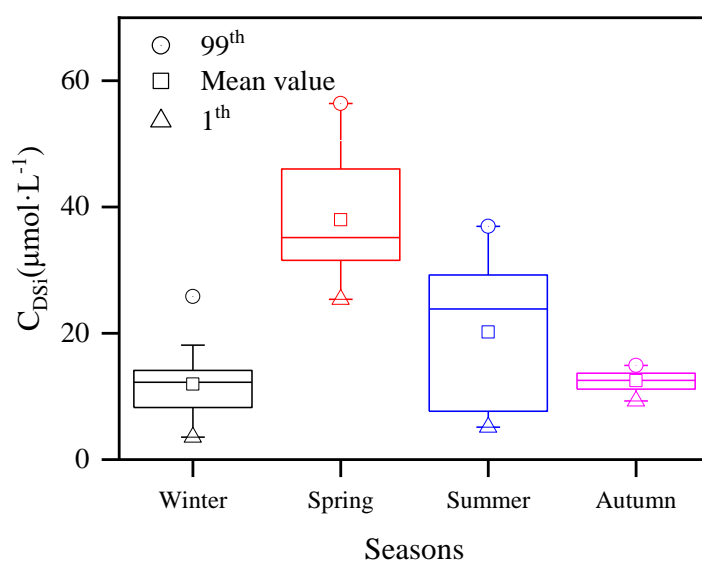


Figure 3. Seasonal changes in DSi illustrated using a box diagram for the coastal water of Zhanjiang Bay.

During the investigation, the concentration of DSi ranged from 3.57 to 56.42 $\mu\text{mol}\cdot\text{L}^{-1}$, with an average of $20.86 \pm 13.14 \mu\text{mol}\cdot\text{L}^{-1}$ in the surface waters of ZJB (Figure 3). The distribution of DSi exhibited a spring maximum and an autumn minimum (November), followed by summer peaks and a secondary winter decline (Figure 3). In addition, the average of DSi concentration was $11.96 \pm 4.85 \mu\text{mol}\cdot\text{L}^{-1}$ with the range of 3.57–25.84 $\mu\text{mol}\cdot\text{L}^{-1}$ in January 2019 (winter). The concentration of DSi ranged from 25.37 to 56.42 $\mu\text{mol}\cdot\text{L}^{-1}$, with an average of $38.00 \pm 9.48 \mu\text{mol}\cdot\text{L}^{-1}$, in April 2019 (spring). In addition, the average of DSi concentration was $20.23 \pm 11.27 \mu\text{mol}\cdot\text{L}^{-1}$, with the range of 5.13–36.96 $\mu\text{mol}\cdot\text{L}^{-1}$, in June 2019 (summer). The average of DSi concentration was $12.48 \pm 1.42 \mu\text{mol}\cdot\text{L}^{-1}$, with the range of 9.30–14.94 $\mu\text{mol}\cdot\text{L}^{-1}$, in November 2019 (autumn).

3.2. Spatiotemporal DSi from Land-Based Sources in ZJB

In this survey, the DSi concentration in the estuaries and sewage outlets around ZJB differed in four seasons (Figure 4). The average DSi concentration was the highest in the normal season, the second highest was in the wet season, while the lowest was in the dry season. The concentration of DSi ranged from 21.52 to 456.80 $\mu\text{mol}\cdot\text{L}^{-1}$ in estuaries and sewage outlets. The concentration of DSi ranged from 29.83 to 281.30 $\mu\text{mol}\cdot\text{L}^{-1}$, with an average of $110.74 \pm 77.98 \mu\text{mol}\cdot\text{L}^{-1}$, in January 2019 (dry season). The average DSi concentration was $159.78 \pm 149.50 \mu\text{mol}\cdot\text{L}^{-1}$, with the range of 21.52–456.80 $\mu\text{mol}\cdot\text{L}^{-1}$, in April (normal season). The concentration of DSi ranged from 42.35 to 333.47 $\mu\text{mol}\cdot\text{L}^{-1}$, with an average of $147.78 \pm 106.00 \mu\text{mol}\cdot\text{L}^{-1}$, in July 2019 (wet season).

The concentration of DSi varied considerably among different estuaries and sewage outlets in ZJB. On the one hand, the highest concentration of DSi in the estuary was 456.80 $\mu\text{mol}\cdot\text{L}^{-1}$, which was located at the Nanliu River estuary (S4), was significantly higher than other sewage outlets. The lowest concentration of DSi was 35.57 $\mu\text{mol}\cdot\text{L}^{-1}$ at the sewage outlet of the flood control sluice in Dengta park (S10). The DSi concentration of the Potou primary school sewage outlet (S11) and Donghai Island aquaculture sewage outlet (S1) were 281.30 and 21.52 $\mu\text{mol}\cdot\text{L}^{-1}$, respectively, which were also the highest and lowest values of the sewage outlets, respectively.

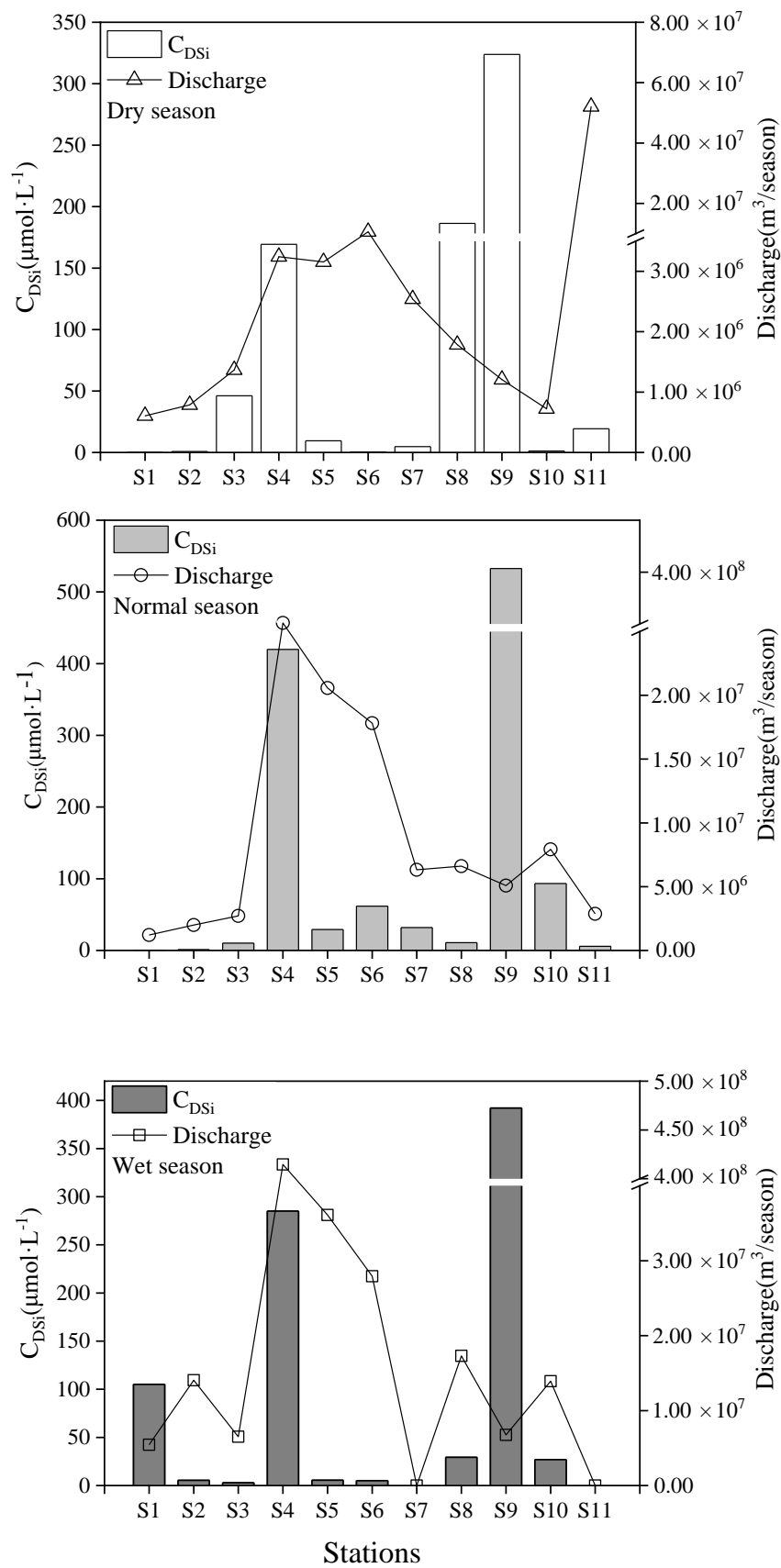


Figure 4. Seasonal concentration (C_{DSi}) and discharge in Zhanjiang Bay.

3.3. Seasonal Flux of DSi in Estuaries and Sewage Outlets Discharging into ZJB

There was considerable variation in the flux of DSi from the 11 land-source monitoring stations during the three water seasons (Figure 5). According to the flux of DSi into the sea in January, April, and July 2019, the flux during the dry season, normal season and wet season of the year were calculated. The annual DSi flux discharged into ZJB was 1.06×10^9 mol, of which 8.28% was in dry season, 41.55% in the normal season and 50.17% in the wet season. The highest flux of DSi was at the mouth of the Suixi River (S9), accounting for 78.94%, 91.53% and 88.77% of the three water seasons, respectively. The flux of DSi in Donghai Island aquaculture sewage outlet (S1) was the lowest during the dry and normal seasons, namely 1.24×10^3 and 3.20×10^3 mol. Compared with the dry season and the normal season, the total amount of DSi flowing into the sea during the wet season increased significantly, reaching 5.32×10^8 mol. The DSi flux was still the highest in the Suixi Estuary (S9), which accounted for 89.10% of the total load, and the flux of DSi in Suixi Estuary (S9) contributed the most to the annual DSi load in ZJB. The flux in the wet season contributed the most to the annual DSi discharge in ZJB, especially the Suixi Estuary S9.

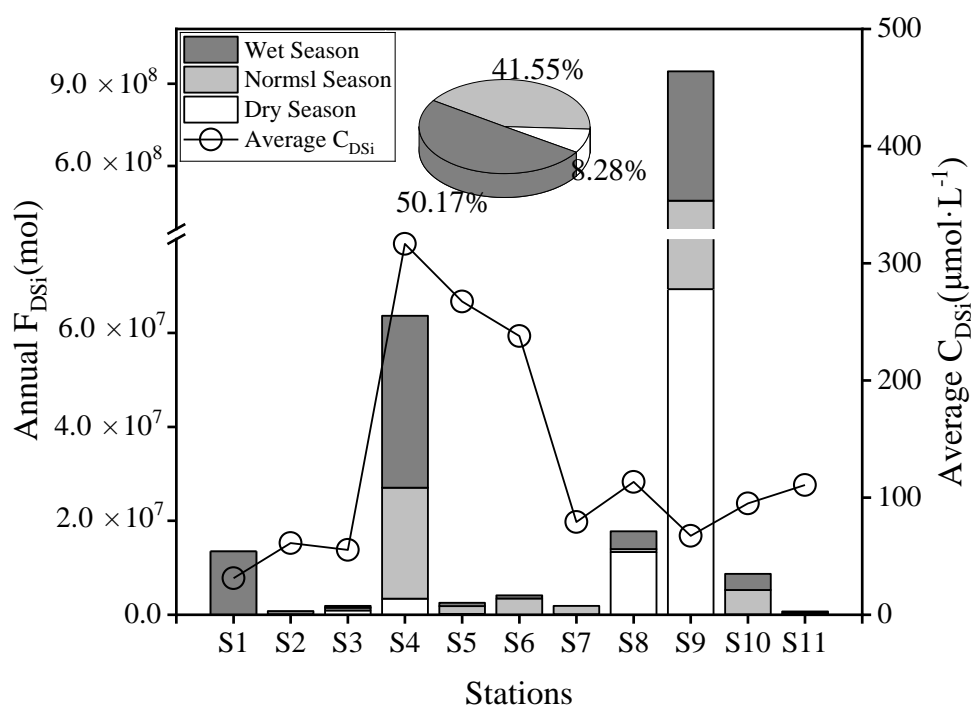


Figure 5. Annual DSi flux (F_{DSi}) and average DSi concentration (C_{DSi}) variation from the estuaries and sewage outlets of Zhanjiang Bay. The pie chart represents the seasonal proportions of F_{DSi} .

3.4. Seasonal Variation of DSi Behaviors in ZJB

Salinity is regarded as a conservative tracer in the ocean except for the dilution of freshwater with seawater [40]. In conservative mixing, the concentration of a nutrient can be expressed as a linear function of salinity along a continuum [26]. The DSi concentration demonstrated relatively conservative mixing behaviors in seasons due to the tidal mixing effect and the riverine inputs (Figure 6). In winter, the DSi concentration was significantly negatively correlated with the range of change in salinity ($R^2 = 0.65$; $p < 0.01$). In spring, the DSi concentration was significantly negatively correlated with salinity ($R^2 = 0.69$; $p < 0.01$). In summer, the DSi concentration was significantly negatively correlated with the narrow range of change in salinity ($R^2 = 0.60$; $p < 0.01$). In autumn, the DSi concentration was significantly negatively correlated with the salinity ($R^2 = 0.49$; $p < 0.01$). In addition, biological uptake of DSi could result in the data falling below the mixing line in different seasons. In comparison,

there were also some data falling above the mixing line, which may be induced by the chemical desorption processes.

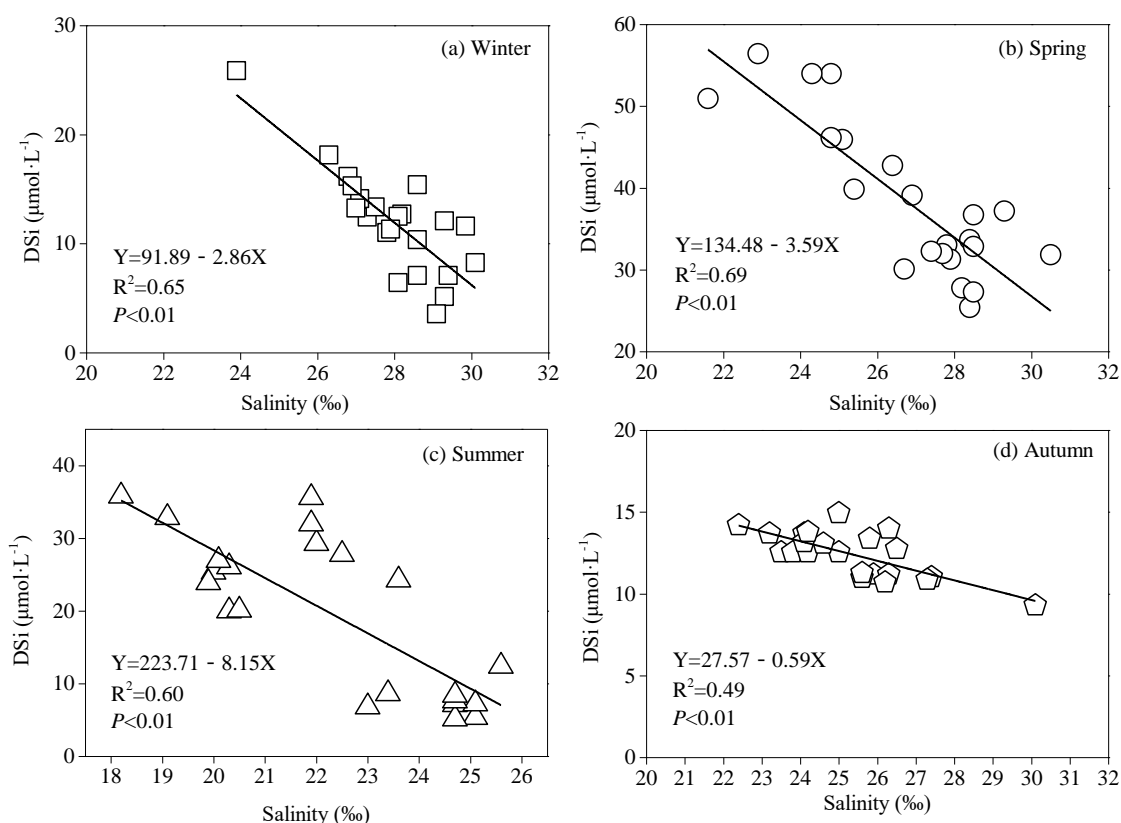


Figure 6. Seasonal variation of DSi behaviors in Zhanjiang Bay.

4. Discussion

4.1. Comparison of DSi Concentration in ZJB with Other Estuaries and Bays around the World

The results show that the surface DSi concentration in ZJB presented obvious spatial and temporal distribution characteristics during the survey period. The results show that the high DSi concentration in different seasons was mainly in April and June 2019, located in the north and northeast of ZJB (Figure 2). Due to the influence of local aquaculture activities, sediment discharge, diatom phytoplankton's influence, microbial growth and metabolism, precipitation and anthropogenic impacts in ZJB, the seasonal DSi variation was significantly different in the coastal waters [42,53]. The range and high value of DSi concentration in ZJB was much lower than in Shenzhen Bay, Hangzhou Bay and Huanghe, but the mean and maximum DSi concentration were higher than those in Rongcheng Bay, the Bay of Bengal, Sanggou Bay, Jiaozhou Bay, Daya Bay, and other coastal waters in China (Table 2) [54–65]. Compared with the Gulf of Finland, the mean DSi concentration was higher in ZJB. However, the range of DSi concentration was lower than in Bothnian Bay in the Baltic Sea [66]. In addition, Chesapeake Bay had a wider range of DSi concentration variation, and DSi concentration in Rhode River in Chesapeake Bay was much greater than mean DSi concentration in land-based sources of ZJB [67,68]. Moreover, the minimum and maximum DSi in ZJB were lower than those in Tokyo Bay and estuary and San Francisco Bay [69,70]. In highly developed bays, such as Shenzhen Bay, Hangzhou Bay, Chesapeake Bay, Tokyo Bay and San Francisco Bay, the DSi had a relatively high concentration, which revealed that anthropogenic activities had impacted on the DSi cycle. In addition, one of the reasons for ZJB is that, as a semi-closed bay, the hydrodynamic exchange conditions are poor due to the impact of reclamation projects, especially in the northern and northeastern waters of the bay [61].

The DSi enrichment in the coastal water was more serious than other sea areas due to the long-term accumulation and non-diffusion of pollution in the sea area. As can be seen from the comparison of DSi concentration between terrestrial sources and seawater in 2019, the variation range of terrestrial DSi concentration was much greater than that of seawater (Table 2). The distribution pattern of DSi was high in summer and autumn, but relatively low in winter. The concentration decreased from the Suixi River estuary to the mouth of ZJB. The variation of DSi concentration in coastal waters was influenced by land-based sources, marine biological processes, and coastal water hydrodynamics. On one hand, the variation of land-source DSi load in ZJB area was different, especially in river and wastewater flow (Figure 3). On the other hand, the hydrodynamics of coastal water played a key role in spatial distribution. In addition, biological activity also changed with the seasons.

Table 2. Comparison of DSi concentration in Zhanjiang Bay (ZJB) with other bays and estuaries.

Study Area	Survey Time	Average Concentration of DSi ($\mu\text{mol}\cdot\text{L}^{-1}$)	Range of DSi Concentration ($\mu\text{mol}\cdot\text{L}^{-1}$)	Reference
Shenzhen Bay	2008	1747 ± 3216	1035–5382	[60]
Rongcheng Bay	2009	6.62	1.36–13.80	[59]
Hangzhou Bay	2006–2007	44.86	11.74–81.59	[55]
Caofeidian coastal water	2013.08–2014.05		0.71–9.52	[62]
Huanghe	2010.04–2011.03	118.10	92.50–146.00	[63]
Sanggou Bay	2003.08–2004.07	2.86	0.07–32.56	[58]
The Yangtze	2005		73–100	[36]
Bay of Bengal	2014		0.6–152.5	[56]
Jiulong River	2013	11.62	0.05–47.81	[64]
Daya Bay	2006.07–2007.11	13.20		[57]
Laizhou Bay	2001	11.31	1.00–52.08	[65]
Jiaozhou Bay	2013–2014		0.71–42.14	[54]
Bothnian Bay	1970–2001	27.62 ± 2.53		[66]
Gulf of Finland	1970–2001	11.82 ± 3.33		[66]
Chesapeake Bay	1984–1988		0.8–93	[67]
Rhode River, Chesapeake Bay	1984–1998 and 1971–1972	270		[68]
Tokyo Bay and estuary	1979–1980		10–300	[69]
San Francisco Bay	1988–2015		25–275	[70]
ZJB (Coastal water)	2019	20.86 ± 13.14	3.57–56.42	This study
ZJB (Land-based sources)	2019	138.89 ± 113.78	21.52–456.80	This study

4.2. Factors Affecting Seasonal Behaviors of DSi in ZJB Coastal Water

In general, there was a significant negative correlation between DSi and salinity, indicating that DSi distribution in ZJB was mainly controlled by physical mixing, while chemical processes and plankton biological activities had little influence on DSi distribution. The river flow component varies considerably, and with it the circulation and salinity patterns in the coastal water. The higher the land-based sources flow, the more conservative the behavior of the DSi profile [7]. In addition, the relative seasonal behaviors of DSi were different, which may be affected by freshwater flow, chemical adsorption or desorption processes and uptake by diatoms [69,70]. On one hand, the river flow significantly decreased, and the flux of DSi entering ZJB also declined in winter. Moreover, the DSi consumption or transfer caused by biological and chemical action was relatively insignificant. In comparison, the land-based flow increased significantly, which resulted in the wide range of salinity variation in summer. The concentration of DSi in the surface of ZJB in summer presents a strong negative correlation with salinity ($R^2 = 0.60$). DSi in coastal water mainly comes from soil weathering and comes from a relatively single source [1]. Although the distribution of nutrients in ZJB and adjacent waters was mainly regulated by physical mixing, sometimes biological and chemical actions in local

waters also become important influencing factors [6,7]. Accompanying the land-based sources' input's seasonal change, the variation of DSi was high in spring and summer, and low in winter and autumn. In summer and spring, the elevated DSi flux may lead to a relatively high DSi concentration in coastal water. Though there was high DSi flux in summer compared with spring, the lower DSi concentration was likely due to biological uptake by diatoms in coastal water [6,7]. It might cause unfavorable conditions for diatom growth and DSi depletion [32]. In addition, the seasonal DSi flux input revealed that land-based sources played a key role in DSi seasonal behaviors. The DSi concentration decreased from the mouth of the Suixi River to the mouth of ZJB. The high positive loading of DSi indicated that rain-driven land-source inputs and organic matter decomposition had an important control effect on DSi in coastal water.

4.3. Factors Affecting DSi Concentration and Flux of Land-based Sources Input in ZJB

Hydrological alterations impacted the DSi concentration and loads to the sea with diverse effects on coastal ecosystem [7,11,20,32]. The flow of DSi varied significantly during the three water seasons (Figure 4). The concentration of DSi was the second largest in the wet season, when there was the highest flow. In contrast, the dry season had the lowest flow and the DSi concentration. The seasonal river discharge was the predominant influencing factor on the seasonal DSi flux. Therefore, the high nutrient loads in the wet season could possibly be attributed to the large freshwater discharges induced by rainfall, especially tropical storms [40,71]. In addition, the Suixi River was the largest contributor of DSi flux discharging into ZJB, which was mainly affected by the agriculture activities and runoff driven by the rainfall [41]. DSi from the chemical weathering of continental rocks was discharged into the ZJB by the largest Suixi River watershed. In contrast, the land-based source (S8) was the sewage outlet of flood control sluice in Binhu park. The flood control sluice was dammed due to anthropogenic activities, which had led to the decline in the water flow discharge and DSi flux. In a former study, it was indicated that *Chaetoceros* was the main phytoplankton species, and a negative relationship between DSi and *Chaetoceros* was observed in ZJB [72]. The seasonal land-based sources of DSi input may inspire diatom bloom, especially in wet seasons. *Skeletonema costatum*, belonging to diatom, had the highest outbreaking frequency, accounted for 43.75% of all outbreaks [43]. The previous study showed that there was high loading of new DSi in periods of high river flow, and more DSi would be available for diatom production and a larger accumulation of diatom biomass in Chesapeake Bay [67]. In periods of low river flow, with low supply rates of new DSi, the magnitude of the accumulation of biomass should be small [67]. Moreover, the concentration of DSi varied considerably among different estuary and sewage outlet among in ZJB, which revealed the different anthropogenic perturbation in the watershed. Under wastewater discharge, some rivers such as Nanliu River, Lvtang, River and Wenbao River had become eutrophic water. A previous study revealed that the process of sewage treatment likely did not remove DSi in the United States [73]. Therefore, the land-based wastewater discharge can also supply the DSi in coastal water, which cannot be neglected in nutrient flux regulation.

4.4. Implications for Seasonal Nutrients Composition in Coastal Waters in ZJB

The level and composition of nutrients played an important role in the growth of phytoplankton in coastal water [40,41]. The Si:N:P ratio of marine diatoms is about 16:16:1 for nutrient-sufficient populations [73–77]. Thus, potential limitation by DSi is indicated by DSi/DIN and DSi/DIP ratios of less than 1 and 16, respectively. Variations in nutrient stoichiometry can have adverse ecological impacts in the coastal water [75–77]. The annual average DSi/DIN and DSi/DIP ratios were 0.44 ± 0.20 and 6.79 ± 2.31 of the coastal water. The DSi/DIN and the DSi/DIP were lower than the Redfield ratio, indicating that the DSi was the limitation nutrient in ZJB (Figure 7). In addition, the DSi/DIN and DSi/DIP ratios were 1.39 ± 1.06 and 23.39 ± 34.67 in the land-based sources, respectively. Additionally, the DSi/DIN and DSi/DIP ratio showed significant seasonal differences ($p < 0.05$). The DSi/DIN ratios were higher in the wet season (0.64 ± 0.19 in coastal water) and normal season (0.44 ± 0.07 in coastal water) compared to the dry season (0.24 ± 0.06 in coastal water), owing to the higher DSi concentration

but relatively lower DIN concentration in the normal and wet seasons. Similarly, the DSi/DIP and DSi/DIN ratios have the same seasonal trend in land-based sources water. The DSi/DIP and DSi/DIN ratios were higher in the wet season (27.97 ± 48.63 and 2.53 ± 1.14 in land-based sources discharge water) and dry season (24.82 ± 35.86 and 1.14 ± 0.68 in land-based sources' discharge water) than in the normal season (18.22 ± 19.41 and 0.69 ± 0.32 in land-based sources' discharge water). Comparatively, the seasonal DSi/DIN and DSi/DIP ratios in land-based sources' discharge water was significantly higher than that in coastal water ($p < 0.05$). The biogeochemical processing together with the inflow composition in the estuaries and sewage outlets can cause an increase in the DSi/DIN and DSi/DIP, which greatly affected nutrient composition in ZJB coastal water. This was one of the possible key reasons that nutrient ratios in coastal water are regulated by riverine input [41]. The increase in DSi/DIN and DSi/DIP induced by land-based sources may be related to eutrophication, increased primary production, and diatom communities blooming in ZJB coastal water. In addition, the increasing phosphorus in ZJB N-limited coastal water may be responsible for the DSi sink. Former studies confirmed that phosphorus enrichment increased diatom production, depleting the reservoir of DSi in the water and leading to DSi-limited diatom growth [13]. Under the silicate biological pump driven by diatoms characterized by fast growth rates and high nutrient demands [2,78], the land-based DSi source input may control the carbon biogeochemical cycle in ZJB.

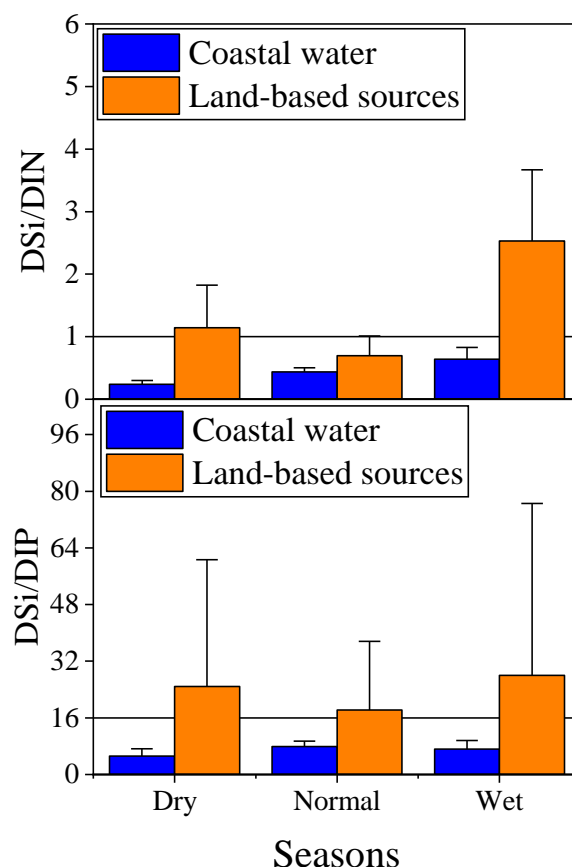


Figure 7. Comparison of DSi/DIN and DSi/DIP between coastal water and land-based sources in Zhanjiang Bay.

5. Conclusions

In summary, our study showed the spatiotemporal DSi variation, sources, and behavior in eutrophic ZJB. The spatial patterns and seasonal variation of DSi had significant differences ($p < 0.05$), reaching $38.00 \pm 9.48 \mu\text{mol}\cdot\text{L}^{-1}$ in spring, $20.23 \pm 11.27 \mu\text{mol}\cdot\text{L}^{-1}$ in summer, $12.48 \pm 1.42 \mu\text{mol}\cdot\text{L}^{-1}$ in autumn and $11.96 \pm 4.85 \mu\text{mol}\cdot\text{L}^{-1}$ in winter, respectively. Additionally, the spatial DSi distribution

showed a decreasing gradient from the top to the mouth of ZJB, which was affected by land-based source inputs and hydrodynamics. Moreover, the concentration and flux of DSi varied considerably among different estuary and sewage outlet in ZJB, which revealed the different anthropogenic perturbation in the river watershed and sewage outlets. The annual DSi flux discharged into ZJB was 1.06×10^9 mol, of which 8.28% was in the dry season, 41.55% was in the normal season and 50.17% was in the wet season, respectively. The highest flux of DSi was located at the mouth of the Suixi River. There were significantly negative correlations between DSi and salinity in all seasons, indicating that DSi distribution in ZJB was typically controlled by physical mixing. The annual average DSi/DIN and DSi/DIP ratios were 0.44 ± 0.20 and 6.79 ± 2.31 in the coastal water. Comparatively, the seasonal DSi/DIN and DSi/DIP ratios in land-based sources' discharge water were significantly higher than those in coastal water ($p < 0.05$). DSi was the limiting nutrient in ZJB, similar to many coastal waters around the world. Seasonal land-based sources' input played an important role in nutrients composition regulation in coastal water that sustained diatoms as the dominant species in ZJB.

Author Contributions: Conceptualization, P.Z.; methodology, P.Z. and J.-B.Z.; software, J.-L.X.; validation, J.-L.X.; Y.L.; J.-X.L.; formal analysis, J.-L.X.; Y.-C.Z.; investigation, J.-B.Z. and P.Z.; resources, P.Z. and J.-B.Z.; data curation, J.-X.L.; X.-Q.L.; writing—original draft preparation, P.Z. and J.-B.Z.; writing—review and editing, P.Z., J.-L.X.; visualization, J.-L.X.; X.-Q.L.; supervision, P.Z. and J.-B.Z.; project administration, P.Z.; J.-B.Z.; funding acquisition, P.Z. and J.-B.Z. All authors have read and agreed to the published version of the manuscript.

Funding: This research was funding by Research and Development Projects in Key Areas of Guangdong Province (2020B111020004); Guangdong Ocean University Ph.D Fund Project (R18021); the Science and Technology Special Project of Zhanjiang city (2019B01081; 2019B01009); First-class Special Fund (231419018); Innovation Strong School Project (230420021) of Guangdong Ocean University.

Acknowledgments: The authors are grateful for the anonymous reviewers' careful review and constructive suggestions to improve the manuscript. Thanks are given to Research and Development Projects in Key Areas of Guangdong Province (2020B111020004); Guangdong Ocean University Ph.D Fund Project (R18021); the Science and Technology Special Project of Zhanjiang city (2019B01081; 2019B01009); First-class Special Fund (231419018); Innovation Strong School Project (230420021) of Guangdong Ocean University.

Conflicts of Interest: The authors declare no conflict of interest.

References

- Carey, J.C.; Fulweiler, R.W. Human activities directly alter watershed dissolved silica fluxes. *Biogeochemistry* **2012**, *111*, 125–138. [[CrossRef](#)]
- Cao, Z.M.; Wang, D.N.; Zhang, Z.L.; Zhou, K.B.; Liu, X.; Wang, L.; Huang, B.Q.; Cai, P.H.; Dai, M.H. Seasonal dynamics and export of biogenic silica in the upper water column of a large marginal sea, the northern South China Sea. *Prog. Oceanogr.* **2020**, *188*, 102421. [[CrossRef](#)]
- DeMaster, D.J. The supply and accumulation of silica in the marine environment. *Geochim. Cosmochim. Acta* **1981**, *45*, 1715–1732. [[CrossRef](#)]
- Papush, L.; Danielsson, Å.; Rahm, L. Dissolved silica budget for the Baltic Sea. *J. Sea. Res.* **2009**, *62*, 31–41. [[CrossRef](#)]
- Kranzler, C.F.; Krause, J.; Brzezinski, M.A.; Edwards, B.R.; Biggs, W.P.; Maniscalco, M.; McCrow, J.; Mooy, B.V.; Bidle, K.; Allen, A.; et al. Silicon limitation facilitates virus infection and mortality of marine diatoms. *Nat. Microbiol.* **2019**, *4*, 1790–1797. [[CrossRef](#)]
- Song, J.M. *Biogeochemical Processes of Biogenic Elements in China Marginal Seas*; Springer: Berlin/Heidelberg, Germany, 2010; pp. 1–662.
- Blanchard, S.F. *Dissolved Silica in the Tidal Potomac River and Estuary, 1979–81 Water Years*; (Water Supply Paper 2234-H); United States Geological Survey: Denver, CO, USA, 1988; p. 46.
- Derry, L.A.; Kurtz, A.C.; Ziegler, K.; Chadwick, O.A. Biological control of terrestrial silica cycling and export fluxes to watersheds. *Nature* **2005**, *433*, 728–731. [[CrossRef](#)]
- Officer, C.; Ryther, J. The possible importance of silicon in marine eutrophication. *Mar. Ecol. Prog. Ser.* **1980**, *3*, 83–91. [[CrossRef](#)]
- Garnier, J.; Beusen, A.; Thieu, V.; Billen, G.; Bouwman, L. N:P:Si nutrient export ratios and ecological consequences in coastal seas evaluated by the ICEP approach. *Glob. Biogeochem. Cycles* **2010**, *24*. [[CrossRef](#)]

11. Carbonnel, V.; Lionard, M.; Muylaert, K.; Lei, C. Dynamics of dissolved and biogenic silica in the freshwater reaches of a macrotidal estuary (The Scheldt, Belgium). *Biogeochemistry* **2009**, *96*, 49–72. [[CrossRef](#)]
12. Wu, B.; Liu, S.M. Dissolution kinetics of biogenic silica and the recalculated silicon balance of the East China Sea. *Sci. Total Environ.* **2020**, *743*. [[CrossRef](#)]
13. Conley, D.J.; Schelske, C.L.; Stoermer, E.F. Modification of the biogeochemical cycle of silica with eutrophication. *Mar. Ecol. Prog. Ser.* **1993**, *101*, 179–192. [[CrossRef](#)]
14. Turner, R.E.; Rabalais, N.N.; Justic, D.; Dortch, Q. Global patterns of dissolved N, P and Si in large rivers. *Biogeochemistry* **2003**, *64*, 297–317. [[CrossRef](#)]
15. Huang, Y.B.; Mi, W.J.; Hu, Z.Y.; Bi, Y.H. Effects of the Three Gorges Dam on spatiotemporal distribution of silicon in the tributary: Evidence from the Xiangxi River. *Environ. Sci. Pollut. Res.* **2019**, *26*, 4645–4653. [[CrossRef](#)] [[PubMed](#)]
16. Song, J.M.; Qu, B.X.; Li, X.G.; Yuan, H.M.; Li, N.; Duan, L.Q. Carbon sinks/sources in the Yellow and East China Seas—Air-sea interface exchange, dissolution in seawater, and burial in sediments. *Sci. China Earth* **2018**, *6*, 1583–1593. [[CrossRef](#)]
17. Tréguer, P.J.; Rocha, C.L.D.L. The world ocean silica cycle. *Annu. Rev. Mar. Sci.* **2013**, *5*, 477–501. [[CrossRef](#)] [[PubMed](#)]
18. Frings, P.J.; Clymans, W.; Fontorbe, G.; de La Rocha, C.L.; Conley, D.J. The continental Si cycle and its impact on the ocean Si isotope budget. *Chem. Geol.* **2016**, *425*, 12–36. [[CrossRef](#)]
19. Sutton, J.N.; André, L.; Cardinal, D.; Conley, D.J.; de Souza, G.F.; Dean, J.; Dodd, J.; Ehlert, C.; Ellwood, M.J.; Frings, P.J. A review of the stable isotope biogeochemistry of the global silicon cycle and its associated trace elements. *Front. Earth Sci.* **2018**, *5*. [[CrossRef](#)]
20. Amann, T.; Weiss, A.; Hartmann, J. Silica fluxes in the inner Elbe estuary, Germany. *Biogeochemistry* **2014**, *118*, 1–24. [[CrossRef](#)]
21. Billen, G.; Lancelot, C.; Meybeck, M. N, P, and Si retention along the aquatic continuum from land to ocean. In *Ocean Margin Processes in Global Change*; Mantoua, R.F.C., Martin, J.M., Wollast, R., Eds.; Wiley: New York, NY, USA, 1991; pp. 19–44.
22. Sun, Y.M.; Song, J.M. Biogeochemistry of nitrogen phosphorus and silicon near the ocean sediment-seawater interface. *Geol. Rev.* **2001**, *47*, 527–534.
23. Durr, H.H.; Meybeck, M.; Hartmann, J.; Laruelle, G.G.; Roubéix, V. Global spatial distribution of natural riverine silica inputs to the coastal zone. *Biogeosciences* **2011**, *8*, 597–620. [[CrossRef](#)]
24. Justic, D.; Rabalais, N.N.; Turner, R.E.; Dortch, Q. Changes in nutrient structure of river-dominated coastal waters: Stoichiometric nutrient balance and its consequences. *Estuar. Coast. Shelf Sci.* **1995**, *40*, 339–356. [[CrossRef](#)]
25. Liu, S.M.; Zhang, J.; Chen, S.Z.; Chen, H.T.; Hong, H.; Wei, H.; Wu, Q.M. Inventory of nutrient compounds in the Yellow Sea. *Cont. Shelf Res.* **2003**, *23*, 1161–1174. [[CrossRef](#)]
26. Robert, G.B. Behaviour of dissolved silica, and estuarine/coastal mixing and exchange processes at Tairua Harbour, New Zealand. *N. Z. J. Mar. Fresh* **1994**, *28*, 55–68.
27. Zhang, J.; Liu, S.M.; Ren, J.L.; Wu, Y.; Zhang, G.L. Nutrient gradients from the eutrophic Changjiang (Yangtze River) Estuary to the oligotrophic Kuroshio waters and revaluation of budgets for the East China Sea Shelf. *Prog. Oceanogr.* **2007**, *74*, 449–478. [[CrossRef](#)]
28. D’Elia, C.F.; Nelson, D.M.; Boynton, W.R. Chesapeake Bay nutrient and plankton dynamics: III. The annual cycle of dissolved silicon. *Geochim. Cosmochim. Ac.* **1983**, *47*, 1945–1955. [[CrossRef](#)]
29. Maavara, T.; Akbarzadeh, Z.; Cappellen, P.V. Global dam-driven changes to riverine N:P:Si ratios delivered to the coastal ocean. *Geophys. Res. Lett.* **2020**, *47*. [[CrossRef](#)]
30. Meunier, J.D.; Braun, J.J.; Riotte, J.; Kumar, C.; Sekhar, M. Importance of weathering and human perturbations on the riverine transport of Si. *Appl. Geochem.* **2011**, *26*, S360–S362. [[CrossRef](#)]
31. Struyf, E.; Smis, A.; van Damme, S.; Garnier, J.; Govers, G.; Van Wesemael, B.; Conley, D.J.; Batelaan, O.; Frot, E.; Clymans, W. Historical land use change has lowered terrestrial silica mobilization. *Nat. Commun.* **2010**, *1*, 129. [[CrossRef](#)]
32. Chen, N.; Wu, Y.; Wu, J.; Yan, X.; Hong, H. Natural and human influences on dissolved silica export from watershed to coast in Southeast China. *J. Geophys. Res. Biogeosci.* **2014**, *119*, 95–109. [[CrossRef](#)]
33. Humborg, C.; Smedberg, E.; Rodriguez-Medina, M.; Mörtz, C.-M. Changes in dissolved silicate loads to the Baltic Sea—The effects of lakes and reservoirs. *J. Mar. Syst.* **2008**, *73*, 223–235. [[CrossRef](#)]

34. Humborg, C.; Ittekkot, V.; Cociasu, A.; Bodungen, B.V. Effect of Danube River dam on Black Sea biogeochemistry and ecosystem structure. *Nature* **1997**, *386*, 385–388. [\[CrossRef\]](#)
35. Humborg, C.; Pastuszak, M.; Aigars, J.; Siegmund, H.; Morth, C.-M.; Ittekkot, V. Decreased silica land–sea fluxes through damming in the Baltic Sea catchment—Significance of particle trapping and hydrological alterations. *Biogeochemistry* **2006**, *77*, 265–281. [\[CrossRef\]](#)
36. Ran, X.B.; Yu, Z.G.; Chen, H.T.; Zhang, X.Q.; Guo, H.B. Silicon and sediment transport of the Changjiang River (Yangtze River): Could the Three Gorges Reservoir be a filter? *Environ. Earth Sci.* **2013**, *70*, 1881–1893.
37. Li, M.T.; Cheng, H.Q. Changes of dissolved silicate flux from the Changjiang River into sea and its influence since late 50 years. *China Environ. Sci.* **2001**, *21*, 193–197.
38. Zhou, Y.P.; Zhang, Y.M.; Li, F.F.; Tan, L.J.; Wang, J.T. Nutrients structure changes impact the competition and succession between diatom and dinoflagellate in the East China Sea. *Sci. Total Environ.* **2017**, *574*, 499–508. [\[CrossRef\]](#) [\[PubMed\]](#)
39. Billen, G.; Garnier, J. River basin nutrient delivery to the coastal sea: Assessing its potential to sustain new production of non-siliceous algae. *Mar. Chem.* **2007**, *106*, 148–160. [\[CrossRef\]](#)
40. Zhang, P.; Ruan, H.M.; Dai, P.D.; Zhao, L.R.; Zhang, J.B. Spatiotemporal river flux and composition of nutrients affecting adjacent coastal water quality in Hainan Island, China. *J. Hydrol.* **2020**, *591*, 125293. [\[CrossRef\]](#)
41. Zhang, P.; Wei, L.R.; Lai, J.Y.; Dai, P.D.; Chen, Y.; Zhang, J.B. Concentration, composition and fluxes of land-based nitrogen and phosphorus source pollutants input into Zhanjiang Bay in Summer. *J. Guangdong Ocean Univ.* **2019**, *39*, 46–55.
42. Zhang, P.; Peng, C.H.; Zhang, J.B.; Zou, Z.B.; Shi, Y.Z.; Zhao, L.R.; Zhao, H. Spatiotemporal urea distribution, sources, and indication of DON bioavailability in Zhanjiang Bay, China. *Water* **2020**, *12*, 633. [\[CrossRef\]](#)
43. Zhang, P.; Peng, C.H.; Zhang, J.B.; Zhang, J.X.; Chen, J.Y.; Zhao, L.R.; Zhao, H. Long-term red tide outbreaks, nutrient pattern under the climate change and anthropogenic pressures in the Zhanjiang Bay, China. 2020; unpublished.
44. Fu, D.; Zhong, Y.; Chen, F.; Yu, G.; Zhang, X. Analysis of dissolved oxygen and nutrients in Zhanjiang Bay and the adjacent sea area in spring. *Sustainability* **2020**, *12*, 889. [\[CrossRef\]](#)
45. Shi, Y.Z.; Zhang, Y.B.; Sun, S.L. Spatiotemporal distribution of eutrophication and its relationship with environmental factors in Zhanjiang Sea Bay Area. *Environ. Sci. Technol.* **2015**, *38*, 90–96, 122.
46. Liu, J.; Zang, J.; Bouwman, L.; Liu, S.; Yu, Z.; Ran, X. Distribution and budget of dissolved and biogenic silica in the Bohai Sea and Yellow Sea. *Biogeochemistry* **2016**, *130*, 85–101. [\[CrossRef\]](#)
47. State Bureau of Quality Technical Supervision. GB17378.4—*The Specification for Marine Monitoring Part 4: Seawater Analysis*; China Standards Press: Beijing, China, 2007.
48. MEPC. *Technical Specifications Requirements for Monitoring of Surface Water and Waste Water*; Standards Press of China: Beijing, China, 2002.
49. Ministry of Water Resources, People's Republic of China. *Code for Liquid Flow Measurement in Open Channels: GB50179-93*; Standards Press of China: Beijing, China, 2005.
50. Liu, S.M.; Ye, X.W.; Zhang, J.; Zhang, G.S.; Wu, Y. The silicon balance in Jiaozhou Bay, North China. *J. Mar. Syst.* **2008**, *74*, 639–648. [\[CrossRef\]](#)
51. Grasshoff, K.; Kremling, K.; Ehrhardt, M. (Eds.) *Methods of Seawater Analysis*, 3rd ed.; Wiley: Weinheim, Germany, 1999.
52. Schlitzer, R. Interactive analysis and visualization of geoscience data with ocean data view. *Comput. Geosci.* **2002**, *28*, 1211–1218. [\[CrossRef\]](#)
53. Zhao, L.R.; Shi, Y.Z.; Zhao, H.; Zhang, J.B.; Sun, X.L. Residues and sources of HCHs and DDTs in the sediments of land-based sewage outlet to the Zhanjiang Bay, China. *Acta Oceanol. Sin.* **2019**, *38*, 8–13. [\[CrossRef\]](#)
54. Gao, L.; Zhang, M.M.; Yao, H.Y.; Liu, Y.L.; Jiang, H.H.; Sha, J.J. An analysis of nutrient structure and limitation changes in Jiaozhou Bay in recent years. *Trans. Oceanol. Limnol.* **2018**, *6*, 61–68.
55. Gao, S.Q.; Chen, J.F.; Jin, H.Y.; Wang, K.; Lu, Y.; Li, H.L.; Chen, F.J. Characteristics of nutrients and eutrophication in the Hangzhou Bay and its adjacent waters. *J. Mar. Sci.* **2019**, *29*, 36–47.
56. Satinder, P.S.; Sunil, K.S.; Ravi, B.; Vinai, K.R. Dissolved silicon and its isotopes in the water column of the Bay of Bengal: Internal cycling versus lateral transport. *Geochim. Cosmochim. Acta* **2015**, *151*, 172–191.
57. Shi, Z.; Huang, X.P. Structure of N, P, Si and their temporal-spatial distribution in Daya Bay, South China. *Mar. Environ. Sci.* **2013**, *32*, 916–921.

58. Sun, P.X.; Zhang, Z.H.; Hao, L.H.; Wang, B.; Wang, Z.L.; Liu, P.; Lian, Y.; Chang, Z.Y.; Xie, L.P. Analysis of nutrient distributions and potential eutrophication in seawater of the Sanggou Bay. *Adv. Mar. Sci.* **2007**, *29*, 436–445.
59. Xie, L.P.; Pu, X.M.; Sun, X.; Wang, B.D. Analysis on the temporal and spatial distribution of nutrients and the influence factors in Rongcheng Bay. *Mar. Sci. Bull.* **2013**, *32*, 19–27.
60. Zhang, J.; Zhang, Y.B.; Zhou, K.; Zhang, J.B.; Sun, X.L. Evaluation on temporal and spatial distribution of nutrients and potential eutrophication in Shenzhen Bay. *Ecol. Environ. Sci.* **2010**, *19*, 253–261.
61. Zhang, Z.F.; Xu, Y.L.; He, J. Influences of long-term reclamation works on hydrodynamic environment in Zhanjiang Bay. *Hydro Sci. Eng.* **2016**, *3*, 96–104.
62. Liu, X.H.; Wang, Y.J.; Shi, Y.J.; Liu, D.Y.; Wang, Y.X.; Tian, H.L.; Cheng, L. Spatial and temporal distribution of nutrients and chlorophyll-a, and their influential factors in Caofeidian coastal waters. *J. Mar. Environ. Sci.* **2020**, *39*, 89–98.
63. Gu, W.Y.; Chen, H.T.; Yao, Q.Z.; Zhang, X.L. Seasonal variation and fluxes of dissolved nutrients in the lower reaches of the Huanghe. *J. Ocean Univ. China* **2017**, *47*, 74–79, 86.
64. Song, X.X.; Yu, Z.M.; Yin, K.D.; Qian, P.Y. Temporal and spatial distribution of nutrients and Chl-a in the coastal area of Hong Kong. *Oceanologia et Limnologia Sinica* **2013**, *44*, 846–852.
65. Sun, P.X.; Wang, B.; Zhang, C.H.; Wang, Z.L.; Xia, B. Relationship between nutrient distributions and eutrophication in seawater of the Laizhou Bay. *J. Adv. Mar. Sci.* **2006**, *24*, 329–335.
66. Papush, L.; Danielsson, Å. Silicon in the marine environment: Dissolved silica trends in the Baltic Sea. *Estuar. Coast. Shelf Sci.* **2006**, *67*, 53–66. [[CrossRef](#)]
67. Conley, D.J.; Malone, T.C. Annual cycle of dissolved silicate in Chesapeake Bay: Implications for the production and fate of phytoplankton biomass. *Mar. Ecol. Prog. Ser.* **1992**, *81*, 121–128. [[CrossRef](#)]
68. Correll, D.L.; Jordan, T.E.; Weller, D. Dissolved silicate dynamics of the Rhode River watershed and estuary. *Estuaries* **2000**, *23*, 188–198. [[CrossRef](#)]
69. Kamatani, A.; Takano, M. The behavior of dissolved silica during the mixing of river and sea waters in Tokyo Bay. *Estuar. Coast. Shelf Sci.* **1984**, *19*, 505–512. [[CrossRef](#)]
70. Cloern, J.E.; Jassby, A.D.; Schraga, T.S.; Nejad, E.; Martin, C. Ecosystem variability along the estuarine salinity gradient: Examples from long-term study of San Francisco Bay. *Limnol. Oceanogr.* **2017**, *62*, S272–S291. [[CrossRef](#)]
71. Kubo, A.; Yamahira, N. Super typhoon induced high silica export from Arakawa River, Japan. *Environ. Sci. Pollut. Res.* **2020**, *27*, 36838–36844. [[CrossRef](#)] [[PubMed](#)]
72. Gong, Y.Y.; Zhang, C.X.; Sun, X.L. Spatiotemporal distribution pattern of Chaetoceros community in Zhanjiang Bay and affecting factors. *Chin. J. Ecol.* **2011**, *30*, 2026–2033.
73. Maguire, T.J.; Fulweiler, R.W. Fate and effect of dissolved silicon within wastewater treatment effluent. *Environ. Sci. Technol.* **2017**, *51*, 7403–7411. [[CrossRef](#)]
74. Redfield, A.C.; Ketchum, B.H.; Richards, F.A. The influence of organisms on the composition of seawater. In *The Sea*; Hill, M.N., Ed.; John Wiley: New York, NY, USA, 1963; Volume 2, pp. 26–77.
75. Brzezinski, M.A. The Si: C: N ratio of marine diatoms: Interspecific variability and the effect of some environmental variables. *J. Phycol.* **1985**, *21*, 347–357. [[CrossRef](#)]
76. Danielsson, Å.; Papush, L.; Rahm, L. Changing the Baltic Sea as a consequence of alterations in nutrient limitations. *J. Mar. Syst.* **2008**, *73*, 263–283. [[CrossRef](#)]
77. Fisher, T.R.; Peele, E.R.; Ammerman, J.W.; Harding, L.W., Jr. Nutrient limitation of phytoplankton in Chesapeake Bay. *Mar. Ecol. Prog. Ser.* **1992**, *82*, 51–63. [[CrossRef](#)]
78. Ragunau, O.; Schultes, S.; Bidle, K.; Claquin, P.; Moriceau, B. Si and C interactions in the world ocean: Importance of ecological processes and implications for the role of diatoms in the biological pump. *Glob. Biogeochem. Cycles* **2006**, *20*, GB4S02. [[CrossRef](#)]

Publisher’s Note: MDPI stays neutral with regard to jurisdictional claims in published maps and institutional affiliations.



© 2020 by the authors. Licensee MDPI, Basel, Switzerland. This article is an open access article distributed under the terms and conditions of the Creative Commons Attribution (CC BY) license (<http://creativecommons.org/licenses/by/4.0/>).